Journal of Zhejiang University-SCIENCE B (Biomedicine & Biotechnology)
ISSN 1673-1581 (Print); ISSN 1862-1783 (Online)
www.jzus.zju.edu.cn; www.springerlink.com
E-mail: jzus@zju.edu.cn

Tissue-engineered composite scaffold of poly(lactide-*co*-glycolide) and hydroxyapatite nanoparticles seeded with autologous mesenchymal stem cells for bone regeneration*

Bing ZHANG[1], Pei-biao ZHANG[2], Zong-liang WANG[2], Zhong-wen LYU[3], Han WU[†‡4]

([1]*Department of Clinical Laboratory, Second Hospital of Jilin University, Changchun 130041, China*)

([2]*Key Laboratory of Polymer Ecomaterials, Changchun Institute of Applied Chemistry, Chinese Academy of Sciences, Changchun 130022, China*)

([3]*Department of Radiology, China-Japan Union Hospital of Jilin University, Changchun 130033, China*)

([4]*Department of Orthopedics, China-Japan Union Hospital of Jilin University, Changchun 130033, China*)

[†]E-mail: drwuhan@163.com

Received Sept. 29, 2016; Revision accepted Feb. 20, 2017; Crosschecked Oct. 20, 2017

Abstract: Objective: A new therapeutic strategy using nanocomposite scaffolds of grafted hydroxyapatite (g-HA)/poly(lactide-*co*-glycolide) (PLGA) carried with autologous mesenchymal stem cells (MSCs) and bone morphogenetic protein-2 (BMP-2) was assessed for the therapy of critical bone defects. At the same time, tissue response and in vivo mineralization of tissue-engineered implants were investigated. Methods: A composite scaffold of PLGA and g-HA was fabricated by the solvent casting and particulate-leaching method. The tissue-engineered implants were prepared by seeding the scaffolds with autologous bone marrow MSCs in vitro. Then, mineralization and osteogenesis were observed by intramuscular implantation, as well as the repair of the critical radius defects in rabbits. Results: After eight weeks post-surgery, scanning electron microscopy (SEM) and energy dispersive X-ray spectroscopy (EDX) revealed that g-HA/PLGA had a better interface of tissue response and higher mineralization than PLGA. Apatite particles were formed and varied both in macropores and micropores of g-HA/PLGA. Computer radiographs and histological analysis revealed that there were more and more quickly formed new bone formations and better fusion in the bone defect areas of g-HA/PLGA at 2–8 weeks post-surgery. Typical bone synostosis between the implant and bone tissue was found in g-HA/PLGA, while only fibrous tissues formed in PLGA. Conclusions: The incorporation of g-HA mainly improved mineralization and bone formation compared with PLGA. The application of MSCs can enhance bone formation and mineralization in PLGA scaffolds compared with cell-free scaffolds. Furthermore, it can accelerate the absorption of scaffolds compared with composite scaffolds.

Key words: Nanocomposite; Surface modification; Bone marrow mesenchymal stem cells; Biomineralization; Bone repair

http://dx.doi.org/10.1631/jzus.B1600412 **CLC number:** R318.08

1 Introduction

The replacement of critical size bone defects due to trauma, tumor resections, or congenital anomalies is a substantial clinical problem in orthopedics and dentistry (Alsberg *et al.*, 2001). Various methods for bone defect treatments have been developed using biological or synthetic grafts (Chen *et al.*, 2011; Huang *et al.*, 2011; Li *et al.*, 2011). In clinic, the gold

‡ Corresponding author

* Project supported by the National Natural Science Foundation of China (Nos. 51473164 and 51273195), the Joint Research Project of Chinese Academy of Sciences and Japan Society for the Promotion of Science (CAS-JSPS; No. GJHZ1519), and the International Science and Technology Cooperation Program of China (No. 2014DFG52510)

ORCID: Bing ZHANG, http://orcid.org/0000-0002-0062-7933; Han WU, http://orcid.org/0000-0002-3409-0046

© Zhejiang University and Springer-Verlag GmbH Germany 2017

standard of grafting material used in bone repairs is autologous bone. Although biological grafts such as autografts, allografts, or xenografts have advantages in biological bone regeneration, their wider application is limited due to histocompatibility, restricted supply, and secondary surgery (Jung *et al.*, 2005). The foundation and rapid development of tissue engineering provides a possible strategy to reconstruct artificial tissue with a three-dimensional (3D) scaffold of biomaterials seeded with cells obtained from a small piece of tissue from the patient (Vacanti *et al.*, 1993; Fuchs *et al.*, 2003; Drosse *et al.*, 2008).

Mesenchymal stem cells (MSCs) have been considered an important cell line for bone tissue engineering, and are capable of undergoing differentiation into a variety of specialized mesenchymal tissues including bone, tendon, cartilage, muscle, ligament, fat, and marrow stroma (Sugiura *et al.*, 2004; Ishikawa *et al.*, 2007). These are prevalent in bone marrow, even in adults, and have been widely used in tissue engineering to promote bone regeneration (Tae *et al.*, 2006; Cordonnier *et al.*, 2010). These cells can be easily isolated and purified from marrow specimens of individuals of any age (Zhou *et al.*, 2008; Katsara *et al.*, 2011), and expanded to over one billion-fold in vitro without any loss in osteogenic potential (Bruder *et al.*, 1997). This property is invaluable for tissue engineering, and allows an individual patient's MSCs to be harvested and expanded in vitro prior to being re-implanted into their body with or without scaffold carriers (Tu *et al.*, 2009).

Bone regeneration in the presence of a synthetic bone graft can take a rather long time for complete anatomical and functional recovery. With this in mind, scientists have focused on higher performance biomaterials in bone tissue engineering to decrease bone healing time (Mastrogiacomo *et al.*, 2006). The recent development of biodegradable synthetic polymers as tissue engineering scaffolds has become an attractive approach for bone repair because of better mechanical properties and unlimited availability. These polymers, mainly polyesters such as poly(L-lactic acid) (PLA), poly(glycolide) (PGA) and their copolymer poly (lactide-*co*-glycolide) (PLGA), have been approved by the US Food and Drug Administration (FDA) for medical applications due to good biocompatibility. On the other hand, as one of the important components in natural bone, hydroxyapatite (HA) ceramics have been used as tissue engineering materials for cell culture and tissue repair because of their biocompatibility and osteoconductivity (Nishikawa *et al.*, 2004). However, the biological activity deficiency of polymers, and the brittleness and fatigue failure in the body of HA ceramics limit their clinical bone repair applications (Cleries *et al.*, 2000). Therefore, the combination of the advantages of these two biomaterials provides a new strategy to improve biological activity and mechanical properties.

Various composite systems of HA with synthetic polymers have been explored as bone substitute materials in recent years, including HA-reinforced PLA (Jeong *et al.*, 2008), collagen (Sena *et al.*, 2009), polyamide (Jie and Li, 2004), poly α-caprolactone (Ciapetti *et al.*, 2003), and poly(α-hydroxyl acids) (Zhang and Ma, 1999). A kind of nano-composite of HA/PLGA fabricated using the gas forming and particulate-leaching (GF/PL) method has been reported (Kim *et al.*, 2006), as well as a 3D fiber-deposited poly(ε-caprolactone)/iron-doped HA nanocomposite magnetic scaffold with tailored mechanical and mass transport properties using rapid prototyping techniques (de Santis *et al.*, 2015), which enhances bone regeneration. However, the problem of interface compatibility for this physical mixture was that it had relatively low uniformity and limited mechanical properties.

In our previous work, we reported a novel composite of grafted HA (g-HA)/poly(L-lactide) (PLLA) (or PLGA) (Hong *et al.*, 2005; 2007). The g-HA was obtained through the hydroxyl groups on the surface of the HA nanoparticles grafted with PLLA, and its blends with PLLA or PLGA were achieved with a higher level of mechanical properties and stability. Furthermore, its cell-free scaffolds have been proven to be mineralizable in vivo and to possess osteogenic ability (Zhang *et al.*, 2009). In the present study, further studies on the application of bone tissue engineering with this composite scaffold were undertaken. According to Drosse *et al.* (2008), the application of growth factors and osteogenic cells has been recommended to improve the recovery quality of large segmental bony defects. Thus, a new therapeutic strategy of nanocomposite scaffolds of g-HA/PLGA carried with autologous MSCs and bone morphogenetic protein-2 (BMP-2) was assessed for the therapy of critical bone defects. At the same time, tissue

response and the in vivo mineralization of tissue-engineered implants were investigated.

2 Materials and methods

2.1 Preparation of foam scaffolds

PLGA (lactic acid/glycolic acid=80/20) was synthesized in our lab by the ring opening copolymerization of the L-lactide and glycolide. HA nanoparticles (100 nm in length and 20–40 nm in width, atomic ratio calcium (Ca)/phosphorous (P)≈1.67) were surface-grafted with PLLA according to the method of our previous study (Hong *et al.*, 2005), and the amount of grafted polymer was approximately 5%–6% (w/w) determined by thermal gravimetric analysis (TGA; TA Instruments TGA500, USA). The nanocomposite of g-HA/PLGA was prepared by 10% (w/w) g-HA, and suspended in 10% (w/v) PLGA/chloroform solution.

The nanocomposite porous scaffold of g-HA/PLGA was fabricated using the solvent casting and particulate-leaching method (Zhang *et al.*, 2009). Briefly, the composite solution was mixed with sucrose particles of 100–450 μm in diameter according to a mass ratio of 1:6, cast in a glass disk, and air-dried for three days. The sucrose particles were subsequently removed from the composites by leaching the composites in distilled water for five days with water changes every 12 h. Then the composites were dried under air and vacuum. Next, the obtained porous scaffolds were cut into small bars (0.3 cm in width, 2.0 cm in length), and sterilized with ultraviolet (UV) for 30 min. The neat PLGA was also fabricated into the scaffold as the control group using the same method. The microstructures of the scaffolds were analyzed using a scanning electron microscope (SEM; XL30 ESEM FEG, PHILIPS).

2.2 Cell isolation and culture

MSCs from rabbit bone marrow were isolated, cultured, and expanded according to the modified procedure described by Roostaeian *et al.* (2006). The 16-week-old adolescent rabbits, weighing (2.96±0.25) kg, were anesthetized, and 2.0 ml of bone marrow was drawn with injectors pre-wetted with 1% fresh heparin at the upper part of tibia of right hind limb. The bone marrow of each rabbit was immediately injected into a 50-ml tube containing 25 ml of serum free medium, dispersed completely, and rinsed with phosphate buffer saline (PBS) three times through 1000 r/min of centrifugation. The obtained cells were resuspended in Dulbecco's modified Eagle's medium (DMEM; Gibco, Rockville, USA) supplemented with 10% fetal bovine serum (FBS; Gibco), 50 mg/L of L-ascorbic acid (Sigma, St. Louis, USA), 10 μg/L of basic fibroblast growth factor (bFGF), 1.0×10^5 U/L of penicillin (Sigma), and 100 mg/L of streptomycin (Sigma). Then cells were plated in tissue culture plates (TCPs; Nunc, Denmark) at a density 2×10^5 cells/ml, and placed in a humidified incubator at 37 °C with 5% CO_2. Non-adherent hematopoietic cells were removed after four days' culture, and the plates were washed gently with culture medium. Thereafter, the medium was changed every two days. Primary MSCs were detached prior to reaching approximately 80% confluence using 0.25% typsin/0.02% ethylenediaminetetraacetic acid (EDTA), and replated at 2×10^4 cells/cm^2. The MSCs were passaged 3–4 times and collected for subsequent experiments.

2.3 Tissue engineering

MSCs were seeded into the porous scaffolds of g-HA/PLGA and PLGA (Zhang *et al*., 2009) using collagen hydrogel as a carrier. A 0.5% (w/w) bovine collagen solution was prepared by dissolving 10 mg of bovine collagen (extracted from the bovine achilles tendon according to (Stone *et al*., 1997)) in 20 ml of 0.1% acetic acid solution at 4 °C. The pH value of the solution was adjusted to 7.0–7.2 with 1 mol/L of NaOH on ice. Then 100 μg/L of human BMP-2 was added. Thereafter, 1 ml of the solution was added into the final concentration of 1×10^7 rabbit MSCs in a tube, and was mixed gently. Half of the collagen/cell mixture with 5×10^6 MSCs was seeded into one of two different materials, and incubated at 37 °C for 10–20 min until the hydrogel formed in the scaffold. Culture was continued for these implants in vitro for three days before implantation. In addition, six of the tissue-engineered implants were prepared and cultured for histological analysis. Two implants were taken out and analyzed with freezing slice and hematoxylin and eosin (H&E) stain.

2.4 Intramuscular implantation

The tissue-engineered porous scaffolds of g-HA/PLGA and PLGA were implanted intramuscularly for

in vivo biodegradation and mineralization assessment. The implants, which were 0.3 cm in width and 2.0 cm in length, were embedded into the dorsal muscle of rabbits by surgery. Three parallel samples from a rabbit were used for each material. After surgery, the rabbits were sacrificed via air injection at the eighth week. The implants were taken out, and macroscopic observation was undertaken and recorded with a digital camera (Fujifilm FinePix S602, Japan). Then the samples were fixed with 4% paraformaldehyde for two hours at room temperature. Three samples of each material at every interval time were washed with distilled water three times and freeze-dried for 48 h for SEM and Ca content analysis.

2.5 Implantation for repair bone defects

The tissue-engineered nanocomposite scaffolds were implanted into the rabbit bone defects, according to Fig. 1. Bilateral and critically sized defects were created in 18 rabbits using a saw and drill in the radius of each rabbit forelimb by removing 2.0 cm of the midshaft diaphyseal bone. The implants of the tissue-engineered scaffolds of g-HA/PLGA and PLGA were seeded with autologous MSCs, cultured for three days, and placed into the defects of different rabbits. The other 12 defects were assigned to the empty defect control. The wounds were closed with silk threads in layers. After the operation, the rabbits were returned to their cages and allowed to move freely. All rabbits were intramuscularly injected with penicillin daily at a dose of 200000 U for three days. All wounds healed gradually, and the rabbits were active without post-surgery complications.

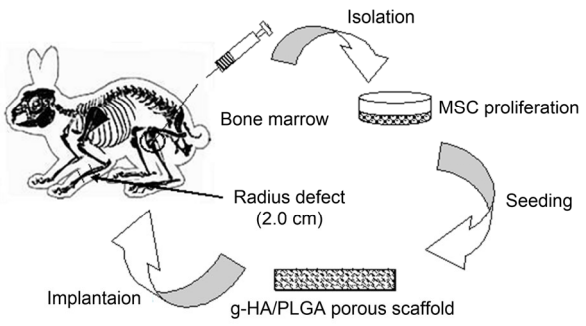

Fig. 1 Scheme of rabbit radius defect replaced with tissue-engineered nanocomposite scaffold of g-HA/PLGA seeded with autologous MSCs

2.6 X-ray examination

The repaired areas at the rabbit radius defects were examined using a computer radiograph (CR; Kodak CR-400plus, USA) at 0-week (first day after surgery), and at 2, 4, and 8 weeks post-surgery. The rabbits were anesthetized and exposed to CR at 120 kV and 200 mA for 32 ms.

2.7 Histological analysis

The rabbits were sacrificed via air injection, and the biopsies of the bone repaired area were obtained at eight weeks post-surgery. The samples were fixed in 4% (w/w) buffered paraformaldehyde for 2–3 d, decalcified in 10% EDTA for approximately four weeks at 37 °C, dehydrated in ascending grades of ethanol, and embedded in paraffin. The tissue blocks were sectioned at 5-mm thicknesses using a microtome (Leica RM2145 Microtome, Germany), and stained with H&E and Masson's trichrome staining.

2.8 RNA isolation and RT-PCR analysis

Total RNA was extracted from the implants and its neighboring muscle tissues using TRIzol reagent (Invitrogen, USA), according to the procedure recommended by the manufacturer. Subsequently, the single stranded complementary DNA (cDNA) was reverse transcribed from 5 μl (20 μg/ml) of total RNA using Moloney murine leukemia virus (M-MLV) reverse transcriptase (TOYOBO, Osaka, Japan), according to the manufacturer's instructions. Both RNA and cDNA concentrations were determined using a Bio-Photometer (Eppendorf, UK).

Semi-quantitative reverse transcription-polymerase chain reaction (RT-PCR) analysis was performed for the rabbit genes of Collagen I, Collagen II, and *Bmp-2* using the primer sequences provided (Table 1), according to the previous method (Li *et al.*, 2005). Briefly, gene specific amplification was conducted by PCR using oligonucleotide primers (Shanghai Sangon, China) as follows: Collagen I, Collagen II, *Bmp-2*, and housekeeping gene glyceraldehyde-3-phosphate dehydrogenase (*Gapdh*) as an internal control. The PCR products were separated with 2% (0.02 g/ml) agarose gel electrophoresis using PowerPac™ Basic (Bio-Rad, USA) and visualized with ethidium bromide (EB) staining. Images were captured and analyzed using the EC3 Imaging System (UVP, USA).

Table 1 Primer sequences used in RT-PCR

Gene	Sequence (5'→3')	Length (bp)
Gapdh	F: GTTTGTGATGGGCGTGAA	664
	R: TCGTCCTCCTCTGGTGCT	
Collagen I	F: CCAGATTGAGACCCTCCTC	652
	R: GGCCAACGTCCACATAGA	
Collagen II	F: GGAAGAGCGGTGACTACTGG	353
	R: GGGCCTTCTTGAGGTTGC	
Bmp-2	F: TTGGAGGAGAAGCAAGGTG	336
	R: CGATGGCATGGTTAGTGG	

F: forward; R: reverse

3 Results

3.1 MSC isolation and proliferation

MSCs of all 18 rabbits were isolated and successfully cultured in vitro. The clones of the primary MSCs were formed at 3–5 d and enlarged rapidly to approximately 80% confluence at 7–9 d (Figs. 2a and 2b). Primary cells were passaged before confluence with a ratio of 1:3 in culture disks. The passaged cells grew more rapidly than the primary cells, and the confluence time was only approximately five days (Fig. 2c). The total time of cell proliferation for each rabbit was approximately 2–3 weeks (3–4 passages) in this study.

3.2 In vivo biodegradation and biomineralization

SEM micrographs of the intramuscular implants of tissue-engineered g-HA/PLGA and PLGA porous scaffolds were taken at eight weeks post-surgery. The images revealed that the artificial bone bonded to the surrounding muscle without any interspace, indicating that the artificial bone has good histocompatibility (Figs. 3a–3d).

EDX analysis was performed to assess the Ca and P content on the surfaces of g-HA/PLGA and PLGA porous scaffolds. These results revealed that the exposure levels of Ca and P on the surface of g-HA/PLGA were higher than those on PLGA (Figs. 3e–3h). However, there was no Ca and only small amounts of P exposure were detected on the surface of PLGA. This indicates that there was increased Ca exposure on the composite surface of g-HA/PLGA to a certain extent due to the surface-grafted HA particles covered with a layer of PLLA, which was embedded in the PLGA matrix for its improved interface between HA and PLGA.

3.3 Bone healing

The critical radius defects of rabbits were implanted with tissue-engineered scaffolds of g-HA/PLGA and PLGA seeded with autologous MSCs. In general, a critical bone defect of 1.5 cm in length cannot be bridged without the assistance of bone implantation or material replacement in the rabbit, or even in the human body (Mokbel *et al.*, 2008). In this study, implants with a length of 2.0 cm, similar to the size of the rabbit radius, were used (Fig. 4a), and these were placed into the defects in the same length without any fixation (Figs. 4c and 4d). The wounds were closed through the routine method of surgery. All rabbits survived after surgery, and the wounds healed in 5–7 d.

3.4 Computer X-ray examination

Fig. 5 shows the radiographs of the repaired areas at the radius defects implanted with the tissue-engineered g-HA/PLGA and PLGA, as well as the control group of the pure defect. In the g-HA/PLGA group, continuous and faint radiographs of new bone

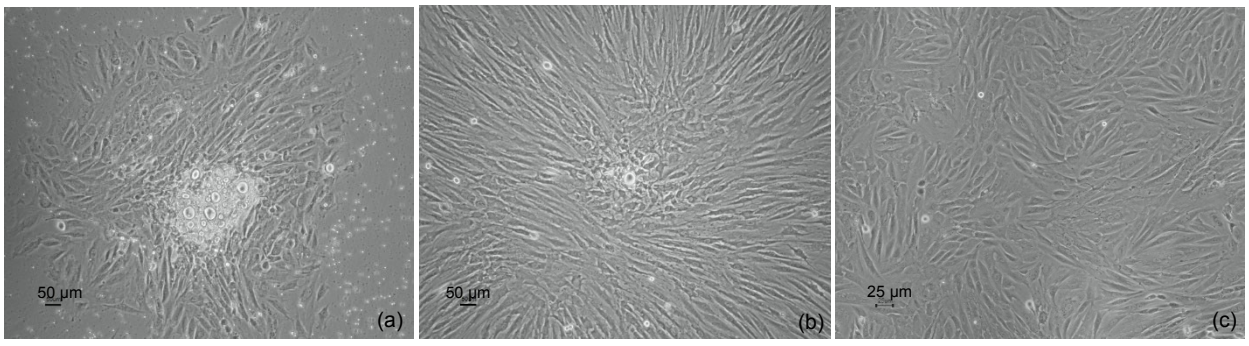

Fig. 2 Cultured autologous MSCs proliferated in vitro
(a) Primary cells were cultured for three days; (b) Primary cells were cultured for one week; (c) Passaged cells grew for three days

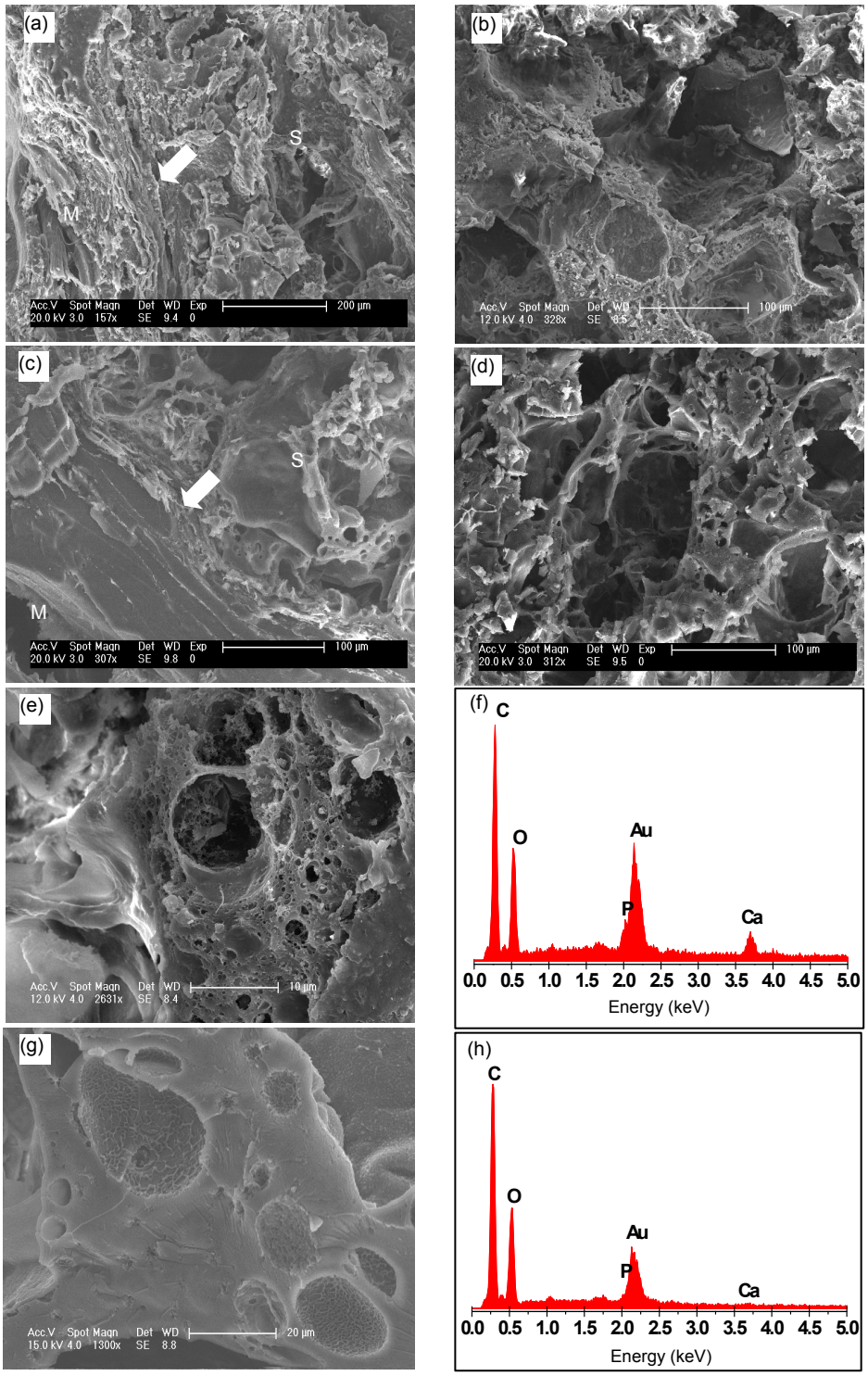

Fig. 3 SEM micrographs and EDX analysis of tissue-engineered intramuscular implants

g-HA/PLGA (a, b) and PLGA (c, d) porous scaffolds at eight weeks post-surgery. Left pictures (a, c) show the adjacent area of the implants to the muscles, and right pictures (b, d) show the center area of the implants. S: area of scaffold implant; M: area of muscle tissue; Arrow: interface between the implant and muscle tissue. Scale bars are 200 μm (a) and 100 μm (b–d). (e, g) Amplificatory SEM micrographs of the areas in (b) and (d) are shown, respectively. (f, h) EDX analyses of (e) and (g), respectively. Scale bars are 10 μm (e) and 20 μm (g)

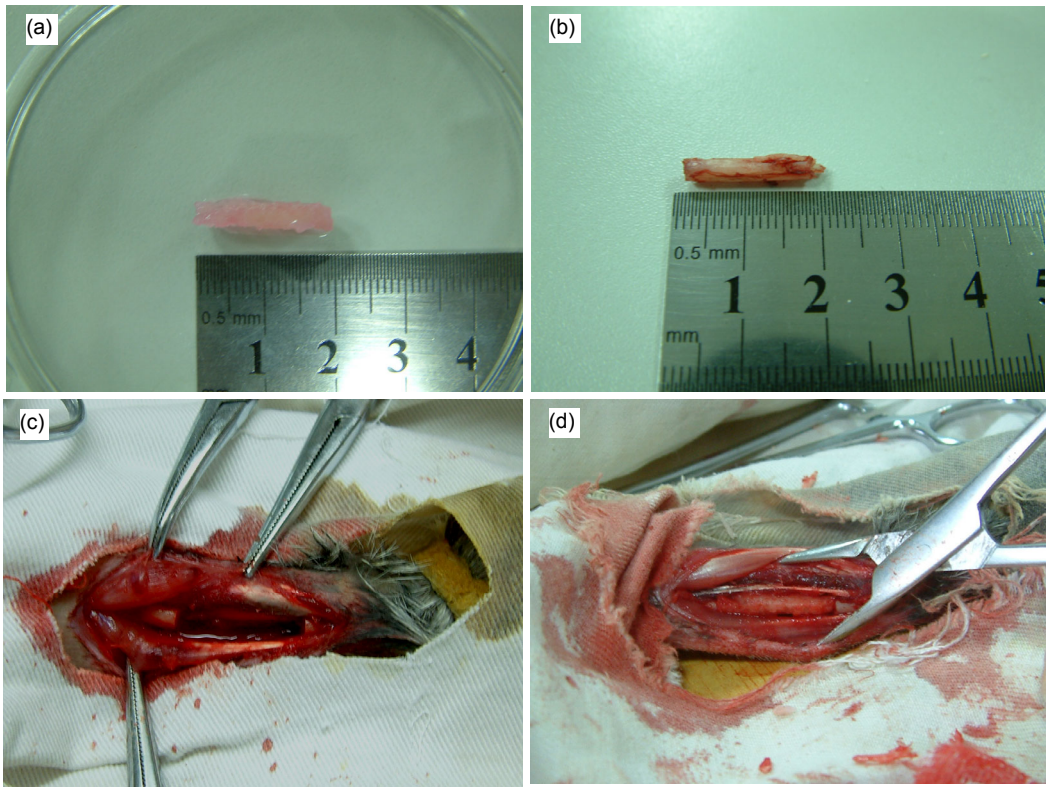

Fig. 4 Macroscopical observation of the tissue-engineered scaffolds

(a) g-HA/PLGA; (b) Bone cut from the rabbit radius; (c) Bone defect model in the 2.0-cm length of the rabbit radius; (d) Tissue-engineered scaffold implanted into the bone defect

formations appeared and filled nearly half of the defect at two weeks post-surgery (Fig. 5b). This became obvious at four weeks due to enhanced mineralization at the repaired area (Fig. 5c). At eight weeks post-surgery, the bone defect was bridged with an intact and newly formed bone. There were smooth appearances at the interfaces between the new bone and neighboring bones (Fig. 5d).

However, in the PLGA group, few new bone formations were found at the defect area near to the neighboring bone at two weeks post-surgery (Fig. 5f). The radiograph at the repaired area was non-continuous, although there was an obvious increase in new bone and its mineralization at four weeks post-surgery (Fig. 5g). At eight weeks post-surgery, the defect in the PLGA group was also bridged due to newly formed bone, but the radiograph appearance only reached a level similar to that of g-HA/PLGA at four weeks (Figs. 5h and 5c). The repaired area and mineralization in PLGA are obviously less than those in g-HA/PLGA at the same time intervals. In the pure defect of the control group, there were extremely few new bone formations at two ends of the defect near the neighboring bone at 2–4 weeks (Figs. 5j and 5k); and this defect could not be bridged at eight weeks due to the limited increase in newly formed bone, and a large defect still remained at the central area (Fig. 5l).

3.5 Histological analysis

Histological analysis was performed of the repaired areas implanted with tissue-engineered g-HA/PLGA and PLGA, and pure defects which underwent H&E staining at eight weeks post-surgery (Fig. 6).

In the g-HA/PLGA group, newly formed bones with intact bone structures appeared at the center of the repaired area (Figs. 6a and 6b). The new bone formation was guided by the scaffold of g-HA/PLGA. There were few fibrous tissues at the interface of the implant and new bones compared to the cell-free scaffold of g-HA/PLGA, which was reported by Wang *et al.* (2016).

SEM analysis revealed the mineral deposits in the interconnected pores and closed pores of the intramuscularly implanted tissue-engineered g-HA/PLGA

Fig. 5 Representative computer X-ray of rabbit critical radius defects implanted with tissue-engineered scaffolds of g-HA/PLGA (a–d) and PLGA (e–h) seeded with autologous MSCs, and the empty defect group (i–l) at 0, 2, 4, and 8 weeks post-surgery

Bone defects in the g-HA/PLGA (d) and PLGA (h) groups were bridged at eight weeks. There were more new bone formations in the g-HA/PLGA group than in the control, PLGA, and empty defect groups. (a, e, i) At 0-week (the first day after surgery); (b, f, j) At two weeks post-surgery; (c, g, k) At four weeks post-surgery; (d, h, and l) At eight weeks post-surgery

for eight weeks (Fig. 7). However, there was a significant difference between these and the only mineralized material nanostructures deposit in micropores, but there are possible complexes of mineralized material with collagen and other extracellular matrix in the interconnected pores. EDX analysis was assessed, and revealed that there was no significant difference in Ca content between the interconnected macropores and closed micropores. We hypothesize that the complexes deposited in the micropores increased and thickened gradually. With material degradation, cracks appeared in the original closed micropores. At the same time, the humor flowed into these and was deposited. Nevertheless, due to the macropore opening, osteoblasts were ingrown, and collagens were bonded with HA. Hence, acicular apatite and collagen are combined to form a scattered composite, which increased gradually and was linked into flakiness. Then these incrassated in sequential horizontal layers.

3.6 RT-PCR analysis

RT-PCR analysis revealed that the mRNA expression of Collagen I, Collagen II and *Bmp-2* in these tissue-engineered implants of g-HA/PLGA at eight weeks post-surgery was more than the expression of these genes in the implant of PLGA at bone defects (Fig. 8).

4 Discussion

A key component in tissue engineering for bone regeneration is the scaffold, which serves as a template for cell interactions and the formation of the bone extracellular matrix, in order to provide structural support to the newly formed tissue (Karageorgiou and Kaplan, 2005). In this study, we developed a novel nanocomposite scaffold of g-HA/PLGA, and its application in bone tissue engineering was investigated with the pure polymer scaffold of PLGA for bone regeneration through tissue engineering technology. At the same time the strategy of applying autologous bone marrow mesenchymal cells in synthetic scaffolds to improve bone formation was assessed.

Scaffolds serve primarily as osteoconductive moieties, since new bone is deposited by creeping substitutions from adjacent living bone (Groeneveld *et al.*, 1999). HA/PLLA composites have shown some advantages in mechanical property, biocompatibility, and osteoconductivity (Hong *et al.*, 2005). In our previous work, a novel nanocomposite of HA grafted

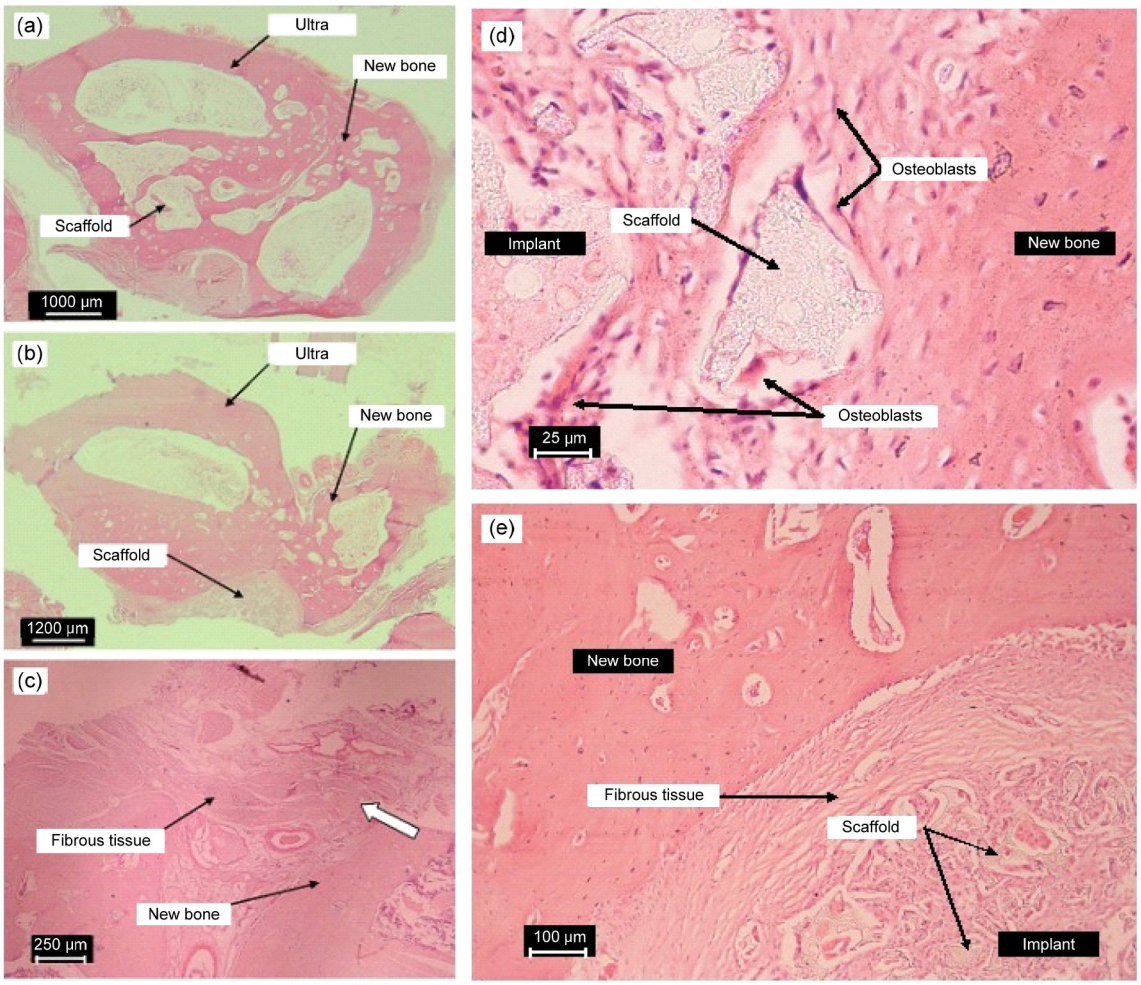

Fig. 6 Representative histological photographs of the repaired areas implanted with tissue-engineered scaffolds of g-HA/PLGA (a) and PLGA (b) with autologous MSCs, and the pure defect (c) at eight weeks post-surgery; typical histological micrographs (d, e) of the interface between the implant and the newly formed bone at eight weeks post-surgery

(a, b) Cross-sections through the center of repaired areas are shown. Photos were taken using a Fujifilm FinePix S602 digital camera with 6× optical zoom. (c) Vertical sections through the pure bone defect with no material replacement are shown. The photos were taken using a light microscope. The samples were decalcified and slices were treated with H&E staining and Masson's trichrome staining. (d) Implant of tissue-engineered g-HA/PLGA, acidophilous osteoclast and basophilic osteoblast. (e) Implant of tissue-engineered PLGA. The gap of the PLGA significantly parceled fibrous tissues. The samples were decalcified and slices were treated with H&E staining and Masson's trichrome staining. Scale bars are 1000 (a), 1200 (b), 250 (c), 25 (d), and 100 (e) μm

with PLLA was obtained, and improved the mechanical property of the blend with PLLA and PLGA to a greater extent (Hong *et al.*, 2005; 2007; Zhang *et al.*, 2009). The composites of g-HA/PLLA (or PLGA) show a wide variety of applications in bone fixing. However, the surface modification of HA particles grafted with PLLA would decrease their Ca exposure to the body to a certain extent (Hong *et al.*, 2004). Hence, this article focused on the further investigation of whether the composite can be employed as a tissue engineering scaffold for bone regeneration.

MSCs have multiple differentiation potentials, and these can be induced to differentiate into bones as seeded cells of tissue engineering artificial bone. In clinic, the bone marrow of a patient can easily be obtained; and isolated MSCs can be used directly in an emergency. In addition, autologous MSCs can be used as seeded cells to avoid immune rejection

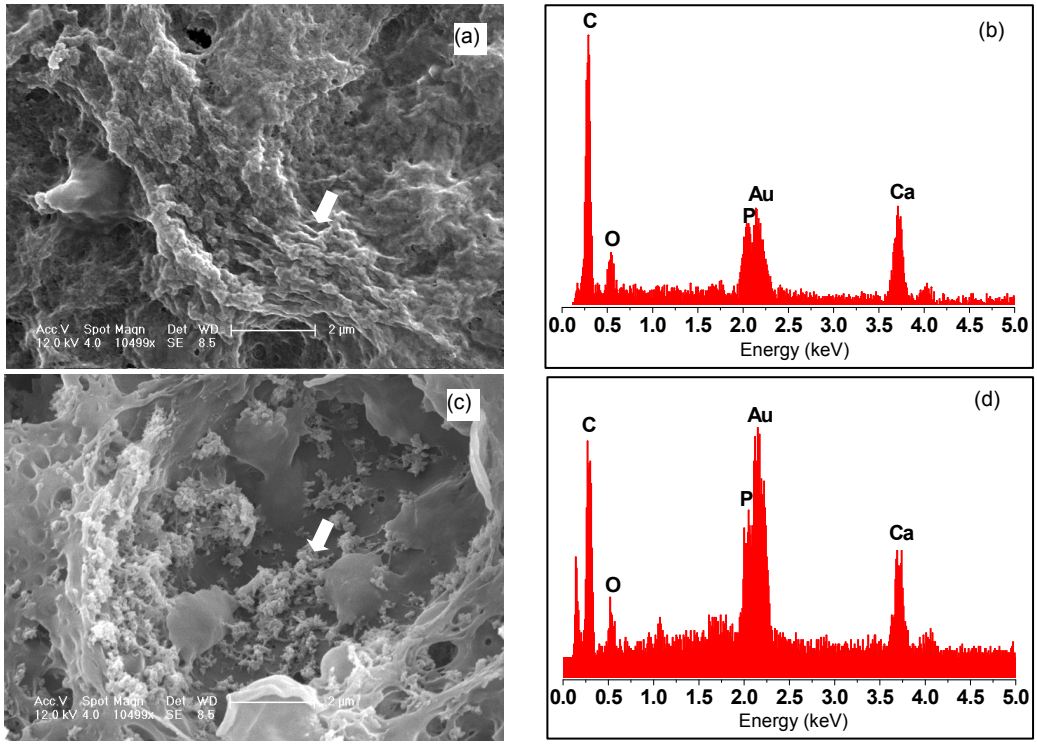

Fig. 7 Comparison of SEM micrographs and EDX element analyses of the mineralized areas in the interconnected macropores (a, b) and the closed micropores (c, d) of the tissue-engineered g-HA/PLGA implanted intramuscularly for eight weeks (b, d)

EDX element analyses of mineralized areas shown by the white arrow in SEM micrographs (a, c). Scale bars are 2 μm (a, c)

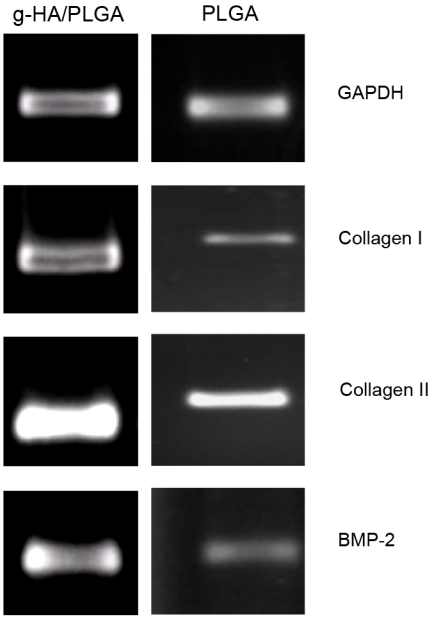

Fig. 8 RT-PCR analysis of the gene expression levels in the tissue-engineered implants of g-HA/PLGA and PLGA at eight weeks post-surgery

mRNA expression of Collagen I, Collagen II, and BMP-2 in the implants of g-HA/PLGA and PLGA at the bone defects is shown

problems, which meets the needs of clinical application. With tissue engineering, the combination of an artificial bone substitute and MSCs would provide a novel method for the therapy of large bone defects, accelerating the clinical process of bone regeneration. In our studies on tissue-engineered artificial bone composite of MSCs with porous scaffolds of g-HA/PLGA and PLGA constructed in vitro, cells grew well in g-HA/PLGA and PLGA scaffolds, and tissue-like structures were formed. It may be that the MSCs derived from the bone marrow are complicated cell lines containing osteogenic cells and other stem cells. It has been reported that the periosteal graft induced cortical bone formation, and the bone marrow graft induced cancellous bone formation with a bone marrow-like structure (Ueno *et al.*, 2008). In another study, it was regarded that the periosteum contributes to radial bone growth by intramembranous ossification (Nakahara *et al.*, 1992). We have demonstrated the presence of surface bone formation around the implant of cell-free PLGA scaffold in our previous

work, which mainly resulted from periosteum creeping and intramembranous ossification (Zhang *et al.*, 2009). However, in this study, mineralization and osteogenics were found in whole implants of g-HA/PLGA. EDX analysis revealed that the levels of Ca and P exposure on the surface of g-HA/PLGA were higher than those on PLGA. In addition, SEM micrographs of the intramuscular implants of tissue-engineered g-HA/PLGA revealed that it has good compatibility with surrounding tissues. These results indicate that tissue engineering technology, where polymer scaffolds are pre-seeded with autologous bone marrow mesenchymal cells cultured in vitro, could improve the osteoconductivity of biomaterials.

In addition to osteoconductivity, scaffolds can serve as delivery vehicles for cytokines such as BMPs, insulin-like growth factors (IGFs), and transforming growth factors (TGFs), which transform recruited precursor cells from the host into bone matrix producing cells (Groeneveld *et al.*, 1999), thereby providing osteoinduction. In our research, we seeded rabbit MSCs to the g-HA/PLGA scaffold by bovine collagen, and BMP-2 was added as follows. We solved the long-term artificial tissue construction problem, where its clinical applications would be affected when rapidly seeding cells to the scaffold. In addition, nutritional support was provided to promote cell proliferation. In normal circumstances, a bone defect longer than 2.0 cm cannot heal naturally, but the new bone can perform the uplift of the callus in both ends of the defect and this can lead to bone nonunion. In this research, in the g-HA/PLGA group, there were continuous and faint radiographs of new bone formation that appeared and filled nearly half of the defect at two weeks post-surgery (Fig. 5b). Up to eight weeks post-surgery, the bone defect was bridged with an intact newly formed bone. There were smooth appearances at the interfaces between the new bone and the neighboring bones (Fig. 5d), and a newly formed bone with an intact bone structure appeared at the center of the repaired area (Figs. 6a and 6b). SEM analysis revealed that mineral deposits in the interconnected pores and closed pores of g-HA/PLGA engineered issues were implanted intramuscularly for eight weeks (Fig. 7). However, there was no significant difference in the content of Ca elements between the interconnected macropores and closed micropores. RT-PCR analysis revealed that the mRNA expression of Collagen I, Collagen II, and *Bmp-2* in the tissue-engineered implants of g-HA/PLGA at eight weeks post-surgery was more than the expression of these genes in the implant of PLGA at the bone defects.

HA has been widely accepted for its bone conduction activity and is often used directly or in conjunction with other materials in clinic. These g-HA/PLGA tissue-engineered artificial bones are constructed by scaffolds. The modified HA nanoparticles can enhance the mechanical properties and stability of the PLGA composite scaffolds, and make the composite scaffold have bone conduction activity by increasing the source of Ca for osteoblast ossification. Simultaneously, the collagen matrix and autologous MSCs can improve the osteogenetic activity of the artificial bone member.

We compared the novel nanocomposite scaffold of g-HA/PLGA with the pure polymer scaffold of PLGA for bone regeneration through tissue engineering. The strategy of autologous bone marrow mesenchymal cells applied in synthetic scaffolds to improve bone formation was also assessed.

In this study, a tissue-engineered implant of nanocomposite scaffold of g-HA/PLGA with autologous MSCs was prepared and applied to repair the critical bone defects of rabbits. MSCs attached and grew well on the surface of the nanocomposite and expressed extracellular matrices (ECMs) in pores. This in vivo implantation study revealed that there was rapid bone formation and bridging at the rabbit radius defect repaired with the tissue-engineered nanocomposite scaffold of g-HA/PLGA. The newly formed bone possessed the intact structure of the long bone and obviously improved osteogenesis.

These results confirmed that the tissue-engineered implant of the nanocomposite scaffold of g-HA/PLGA with autologous MSCs can significantly enhance bone regeneration and repair capability, and accelerate bone fusion defect rates. In addition, the repair effect was significantly better than tissue-engineered artificial bones of pure PLGA. Thus, the tissue-engineered artificial bone with autologous living cells prepared by the investigators could be used as alternatives to autogenous bone graft, and has broad application prospects in clinical bone defect transplant repair.

5 Conclusions

The incorporation of g-HA was mainly carried out to improve mineralization and bone formation compared with PLGA. First, it enhanced the binding ability of the scaffold and bone, reducing the formation of fibrous wrapping tissues. In addition, it facilitated the formation and deposit of minerals, which is beneficial to the expression of bone-related genes and osteoblast differentiation, as well as bone formation. The application of MSCs enhanced bone formation and the mineralization of the PLGA scaffold, compared with cell-free scaffolds. In addition, it accelerated the absorption of the scaffold compared to composite scaffolds. However, there was no significant effect on the bone mass of osteogenesis. A large number of osteoblasts existed in the local experimental bone defect.

Contributors

Bing ZHANG and Zong-liang WANG performed the experiments, analyzed data, and wrote the manuscript; Pei-biao ZHANG and Han WU provided guidance, analyzed data, and revised the manuscript; Zhong-wen LYU designed the study and provided X-ray and analyzed data.

Compliance with ethics guidelines

Bing ZHANG, Pei-biao ZHANG, Zong-liang WANG, Zhong-wen LYU, and Han WU declare that they have no conflict of interest.

All institutional and national guidelines for the care and use of laboratory animals were followed.

References

Alsberg, E., Anderson, K.W., Albeiruti, A., *et al*., 2001. Cell-interactive alginate hydrogels for bone tissue engineering. *J. Dent. Res*., **80**(11):2025-2029. http://dx.doi.org/10.1177/00220345010800111501

Bruder, S.P., Jaiswal, N., Haynesworth, S.E., 1997. Growth kinetics, self-renewal, and the osteogenic potential of purified human mesenchymal stem cells during extensive subcultivation and following cryopreservation. *J. Cell Biochem*., **64**(2):278-294. http://dx.doi.org/10.1002/(SICI)1097-4644(199702)64

Chen, W.C., Anderson, K.W., Albeiruti, A., *et al*., 2011. Evaluating osteochondral defect repair potential of autologous rabbit bone marrow cells on type II collagen scaffold. *Cytotechnology*, **63**(1):13-23. http://dx.doi.org/10.1007/s10616-010-9314-9

Ciapetti, G., Ambrosio, L., Savarino, L., *et al*., 2003. Osteoblast growth and function in porous poly epsilon-caprolactone matrices for bone repair: a preliminary study. *Biomaterials*, **24**(21):3815-3824. http://dx.doi.org/10.1016/S0142-9612(03)00263-1

Cleries, L., Fernandez-Pradas, J.M., Morenza, J.L., 2000. Behavior in simulated body fluid of calcium phosphate coatings obtained by laser ablation. *Biomaterials*, **21**(18):1861-1865. http://dx.doi.org/10.1016/S0142-9612(00)00060-0

Cordonnier, T., Layrolle, P., Gaillard, J., *et al*., 2010. 3D environment on human mesenchymal stem cells differentiation for bone tissue engineering. *J. Mater. Sci. Mater. Med.*, **21**(3):981-987. http://dx.doi.org/10.1007/s10856-009-3916-9

de Santis, R., Russo, A., Gloria, A., *et al*., 2015. Towards the design of 3D fiber-deposited poly(ε-caprolactone)/iron doped hydroxyapatite nanocomposite magnetic scaffolds for bone regeneration. *J. Biomed. Nanotechnol.*, **11**(7):1236-1246. http://dx.doi.org/10.1166/jbn.2015.2065

Drosse, I., Volkmer, E., Capanna, R., *et al*., 2008. Tissue engineering for bone defect healing: an update on a multi-component approach. *Injury*, **39**(Suppl. 2):S9-S20. http://dx.doi.org/10.1016/S0020-1383(08)70011-1

Fuchs, J.R., Hannouche, D., Terada, S., *et al*., 2003. Fetal tracheal augmentation with cartilage engineered from bone marrow-derived mesenchymal progenitor cells. *J. Pediatr. Surg.*, **38**(6):984-987. http://dx.doi.org/10.1016/S0022-3468(03)00139-8

Groeneveld, E.H., van den Bergh, J.P., Holzmann, P., *et al*., 1999. Mineralization processes in demineralized bone matrix grafts in human maxillary sinus floor elevations. *J. Biomed. Mater. Res.*, **48**(4):393-402. http://dx.doi.org/10.1002/(SICI)1097-4636(1999)48:4<393::AID-JBM1>3.3.CO;2-3

Hong, Z.K., Qiu, X.Y., Sun, J.R., *et al*., 2004. Grafting polymerization of L-lactide on the surface of hydroxyapatite nano-crystals. *Polymer*, **45**(19):6699-6706. http://dx.doi.org/10.1016/j.polymer.2004.07.036

Hong, Z.K., Zhang, P.B., He, C.L., *et al*., 2005. Nano-composite of poly(L-lactide) and surface grafted hydroxyapatite: mechanical properties and biocompatibility. *Biomaterials*, **26**(32):6296-6304. http://dx.doi.org/10.1016/j.biomaterials.2005.04.018

Hong, Z.K., Zhang, P.B., Liu, A.X., *et al*., 2007. Composites of poly(lactide-*co*-glycolide) and the surface modified carbonated hydroxyapatite nanoparticles. *J. Biomed. Mater. Res. A*, **81A**(3):515-522. http://dx.doi.org/10.1002/jbm.a.31038

Huang, J., Yao, C.L., Wei, Y.H., *et al*., 2011. Repair of bone defect in caprine tibia using a laminated scaffold with bone marrow stromal cells loaded poly(L-lactic acid)/β-tricalcium phosphate. *Artif. Organs*, **35**(1):49-57. http://dx.doi.org/10.1111/j.1525-1594.2010.01042.x

Ishikawa, H., Kitoh, H., Sugiura, F., *et al*., 2007. The effect of recombinant human bone morphogenetic protein-2 on the osteogenic potential of rat mesenchymal stem cells after

several passages. *Acta Orthop.*, **78**(2):285-292. http://dx.doi.org/10.1080/17453670710013816

Jeong, S.I., Ko, E.K., Yum, J., *et al*., 2008. Nanofibrous poly(lactic acid)/hydroxyapatite composite scaffolds for guided tissue regeneration. *Macromol. Biosci.*, **8**(4):328-338. http://dx.doi.org/10.1002/mabi.200700107

Jie, W., Li, Y., 2004. Tissue engineering scaffold material of nano-apatite crystals and polyamide composite. *J. Eur. Polym.*, **40**(3):509-515. http://dx.doi.org/10.1016/j.eurpolymj.2003.10.028

Jung, Y., Kim, S.S., Kim, Y.H., *et al*., 2005. A poly(lactic acid)/calcium metaphosphate composite for bone tissue engineering. *Biomaterials*, **26**(32):6314-6322. http://dx.doi.org/10.1016/j.biomaterials.2005.04.007

Karageorgiou, V., Kaplan, D., 2005. Porosity of 3D biomaterial scaffolds and osteogenesis. *Biomaterials*, **26**(27): 5474-5491. http://dx.doi.org/10.1016/j.biomaterials.2005.02.002

Katsara, O., Mahaira, L.G., Iliopoulou, E.G., *et al*., 2011. Effects of donor age, gender, and in vitro cellular aging on the phenotypic, functional, and molecular characteristics of mouse bone marrow-derived mesenchymal stem cells. *Stem Cells Dev.*, **20**(9):1549-1561. http://dx.doi.org/10.1089/scd.2010.0280

Kim, S.S., Sun Park, M., Jeon, O., *et al*., 2006. Poly(lactide-*co*-glycolide)/hydroxyapatite composite scaffolds for bone tissue engineering. *Biomaterials*, **27**(8):1399-1409. http://dx.doi.org/10.1016/j.biomaterials.2005.08.016

Li, J., Hong, J., Zheng, Q., *et al*., 2011. Repair of rat cranial bone defects with nHAC/PLLA and BMP-2-related peptide or rhBMP-2. *J. Orthop. Res.*, **29**(11):1745-1752. http://dx.doi.org/10.1002/jor.21439

Li, W.J., Tuli, R., Okafor, C., *et al*., 2005. A three-dimensional nanofibrous scaffold for cartilage tissue engineering using human mesenchymal stem cells. *Biomaterials*, **26**(6): 599-609. http://dx.doi.org/10.1016/j.biomaterials.2004.03.005

Mastrogiacomo, M., Scaglione, S., Martinetti, R., *et al*., 2006. Role of scaffold internal structure on in vivo bone formation in macroporous calcium phosphate bioceramics. *Biomaterials*, **27**(17):3230-3237. http://dx.doi.org/10.1016/j.biomaterials.2006.01.031

Mokbel, N., Bou Serhal, C., Matni, G., *et al*., 2008. Healing patterns of critical size bony defects in rat following bone graft. *Oral Maxillofac. Surg.*, **12**(2):73-78. http://dx.doi.org/10.1007/s10006-008-0107-7

Nakahara, H., Goldberg, V.M., Caplan, A.I., 1992. Culture-expanded periosteum-derived cells exhibit osteochondrogenic potential in porous calcium phosphate ceramics in vivo. *Clin. Orthop.*, **276**:291-298.

Nishikawa, M., Myoui, A., Ohgushi, H., *et al*., 2004. Bone tissue engineering using novel interconnected porous hydroxyapatite ceramics combined with marrow mesenchymal cells: quantitative and three-dimensional image analysis. *Cell Transplant.*, **13**(4):367-376. http://dx.doi.org/10.3727/000000004783983819

Roostaeian, J., Carlsen, B., Simhaee, D., *et al*., 2006. Characterization of growth and osteogenic differentiation of rabbit bone marrow stromal cells. *J. Surg. Res.*, **133**(2):76-83. http://dx.doi.org/10.1016/j.jss.2005.09.026

Sena, L.A., Caraballo, M.M., Rossi, A.M., *et al*., 2009. Synthesis and characterization of biocomposites with different hydroxyapatite-collagen ratios. *J. Mater. Sci. Mater. Med.*, **20**(12):2395-2400. http://dx.doi.org/10.1007/s10856-009-3813-2

Stone, K.R., Steadman, J.R., Rodkey, W.G., *et al*., 1997. Regeneration of meniscal cartilage with use of a collagen scaffold. Analysis of preliminary data. *J. Bone Joint Surg. Am.*, **79**(12):1770-1777. http://dx.doi.org/10.2106/00004623-199712000-00002

Sugiura, F., Kitoh, H., Ishiguro, N., 2004. Osteogenic potential of rat mesenchymal stem cells after several passages. *Biochem. Biophys. Res. Commun.*, **316**(1):233-239. http://dx.doi.org/10.1016/j.bbrc.2004.02.038

Tae, S.K., Lee, S.H., Park, J.S., *et al*., 2006. Mesenchymal stem cells for tissue engineering and regenerative medicine. *Biomed. Mater.*, **1**(2):63-71. http://dx.doi.org/10.1088/1748-6041/1/2/003

Tu, J., Wang, H., Li, H., *et al*., 2009. The in vivo bone formation by mesenchymal stem cells in zein scaffolds. *Biomaterials*, **30**(26):4369-4376. http://dx.doi.org/10.1016/j.biomaterials.2009.04.054

Ueno, T., Honda, K., Hirata, A., *et al*., 2008. Histological comparison of bone induced from autogenously grafted periosteum with bone induced from autogenously grafted bone marrow in the rat calvarial defect model. *Acta Histochem.*, **110**(3):217-223. http://dx.doi.org/10.1016/j.acthis.2007.10.008

Vacanti, C.A., Kim, W., Upton, J., *et al*., 1993. Tissue-engineered growth of bone and cartilage. *Transplant. Proc.*, **25**(1 Pt 2):1019-1021.

Wang, Z., Yu, Y., Wang, Y., *et al*., 2016. Enhanced in vitro mineralization and in vivo osteogenesis of composite scaffolds through controlled surface grafting of L-actic acid oligomer on nanohydroxyapatite. *Biomacromolecules*, **17**(3):818-829. http://dx.doi.org/10.1021/acs.biomac.5b01543

Zhang, P., Hong, Z., Yu, T., *et al*., 2009. In vivo mineralization and osteogenesis of nanocomposite scaffold of poly (lactide-*co*-glycolide) and hydroxyapatite surface-grafted with poly(L-lactide). *Biomaterials*, **30**(1):58-70. http://dx.doi.org/10.1016/j.biomaterials.2008.08.041

Zhang, R., Ma, P.X., 1999. Poly(α-hydroxyl acids)/hydroxyapatite porous composites for bone-tissue engineering. I. Preparation and morphology. *J. Biomed. Mater. Res.*, **44**(4): 446-455. http://dx.doi.org/10.1002/(SICI)1097-4636(19990315)44:4<446::AID-JBM11>3.0.CO;2-F

Zhou, S., Greenberger, J.S., Epperly, M.W., *et al*., 2008. Age-related intrinsic changes in human bone-marrowderived mesenchymal stem cells and their differentiation to osteoblasts. *Aging Cell*, **7**(3):335-343.

中文概要

题　目：组织工程复合支架聚乳酸-羟基乙酸共聚物和羟基磷灰石纳米粒子接种自体骨髓间充质干细胞应用于骨再生

目　的：对应用接枝的羟基磷灰石（g-HA）/聚乳酸-羟基乙酸共聚物（PLGA）纳米复合支架接种自体骨髓间充质干细胞（MSCs）和骨形态发生蛋白 2（BMP-2）治疗重症骨缺损的新的治疗策略进行评估，并通过肌肉内移植研究人工骨的组织相容性和移植物在体内的矿化和缺损骨的愈合。

创新点：改性的 PLGA 接种自体 MSCs 的组织工程骨加速了骨缺损的愈合，使临床重症骨缺损的治疗有了新的手段。

方　法：应用溶剂浇铸和粒子沥滤方法将 PLGA 和 g-HA 制备成复合支架 g-HA/PLGA。在 g-HA/PLGA 支架上接种兔自体 MSCs 制成组织工程移植物。取宽 0.3 cm 长 2.0 cm 的上述移植物埋入兔背部肌肉内，8 周后取出移植物，使用扫描式电子显微镜（SEM）检测人工骨的组织相容性（图 3a），X 射线能量色散谱（EDX）分析钙浓度。然后，用锯锯掉兔前肢桡骨骨干 2.0 cm，取同样长度的上述移植物放置于骨缺损处（图 4）。术后 2、4、8 周应用计算机 X 线摄影（CR）检测骨缺损愈合情况（图 5），组织学分析愈合组织结构（图 6），SEM 检测人工骨与周围组织的相容性（图 7），反转录聚合酶链式反应（RT-PCR）检测愈合组织 Collagen I、Collagen II 和 *Bmp-2* 基因的表达。

结　论：PLGA 掺入 g-HA 主要改善了矿化作用，有益于骨相关基因的表达和骨形成。自体 MSCs 的应用增强了骨形成和 PLGA 支架的矿化作用，并加速了支架的吸收。

关键词：纳米颗粒；表面改性；骨髓间充质干细胞；生物矿化；骨修复